A software prototype for assessing the reliability of a concrete bridge superstructure subjected to chloride-induced reinforcement corrosion

Ronald Schneider
BAM Federal Institute for Materials Research and Testing, Berlin, Germany

Sebastian Thöns
Technical University of Denmark, Lyngby, Denmark

Johannes Fischer, Maximilian Bügler, André Borrmann & Daniel Straub
Technische Universität München, Germany

ABSTRACT: A software prototype is developed for assessing and updating the reliability of single-cell prestressed concrete box girders subjected to chloride-induced reinforcement corrosion. The underlying system model consists of two integrated sub-models: a condition model for predicting the deterioration state of the box girder and a structural model for evaluating the overall system reliability. The condition model is based on a dynamic Bayesian network (DBN) model which considers the spatial variation of the corrosion process. Inspection data are included in the calculation of the system reliability through Bayesian updating on the basis of the dynamic DBN model. To demonstrate the effect of partial inspections, the software prototype is applied to a case study of a typical highway bridge with six spans. The case study illustrates that it is possible to infer the condition of uninspected parts of the structure due to the spatial correlation of the corrosion process.

1 INTRODUCTION

Prestressed concrete bridges are an important part of road infrastructures. They are generally subjected to deterioration processes including corrosion and fatigue of the reinforcement and prestressing tendons. These deterioration processes are subject to large uncertainties and they reduce the reliability of concrete bridges. To reduce the uncertainty on the actual condition of deteriorating concrete bridges, inspections may be performed. Based on their results, repair and maintenance actions can be planned.

Dynamic Bayesian networks (DBN) are a computational framework suitable for modeling stochastic deterioration processes (Straub, 2009). Bayesian updating of deterioration models with monitoring and inspections results can be performed robustly and efficiently on the basis of DBN. The DBN framework is therefore ideally suited for developing software for the management of deteriorating structures that can be used by engineers who are not experts in reliability analysis.

To prove the concept, a software prototype for assessing and updating the reliability of single-cell prestressed concrete box girders subjected to chloride-induced reinforcement corrosion has been developed. Section 2 gives an overview on the underlying system model. The specific sub-models are described in more detail in Sections 3 and 4. Note that the paper does not provide an introduction to DBN. The reader is referred to (Murphy, 2002) and (Straub, 2009) for more details. The implementation of the prototype is briefly described in Section 5. A case study applying the prototype is summarized in Section 6.

2 SYSTEM MODEL

To model the deterioration state, the single-cell prestressed concrete box girder is divided into n sections as indicated in Figure 1. Each section i is further divided into four elements: the deck plate, the bottom flange, and both webs. The deterioration state of each element at time t is described by a set of random variables. This includes a variable representing the relative corrosion progress as described in Section 3. It is assumed that the deterioration state within an element j is constant, i.e. a relative corrosion progress of 0.05 represents an area reduction of the entire reinforcement associated with element j by 5%.

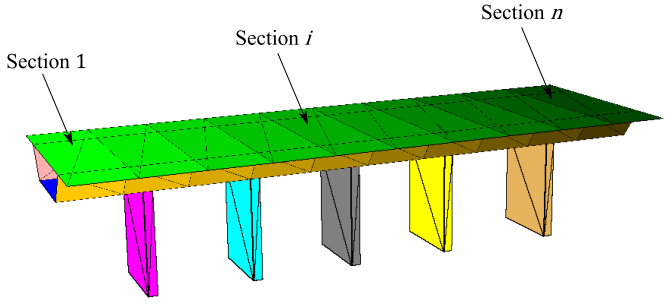

Figure 1. Sections defining the element size of the deterioration model of the box girder. Each section consists of four elements: a deck plate, a bottom flange and two webs.

All random variables describing the deterioration state of the individual elements at time t are collected in a vector $\boldsymbol{\Psi}_t = \boldsymbol{\Psi}(t)$ representing the overall deterioration state of the box girder. The joint distribution $p(\boldsymbol{\psi}_t)$ of $\boldsymbol{\Psi}_t$ is computed based on a DBN model of the corrosion process, which considers the spatial correlation among the deterioration in individual elements. This model is described in more detail in Section 3.

Following Straub and Der Kiureghian (2011), the deterioration state of the box girder is considered constant over a period $\Delta t = 1$ year. Conservatively, the deterioration state of the box girder in the period $[t - \Delta t, t]$ is set equal to the state at time t, $\boldsymbol{\Psi}_t$. The event of structural collapse of the box girder in that time interval is denoted by $F_t = F(t)$. The probability of structural collapse conditional on the deterioration state of the box girder at time t, $\Pr(F_t|\boldsymbol{\Psi}_t = \boldsymbol{\psi}_t)$, is computed by means of a probabilistic structural model of the box girder. This model is described in more detail in Section 4.

The overall probability of structural collapse in the period $[t - \Delta t, t]$ is given by the total probability theorem as:

$$\Pr(F_t) = \sum_{\boldsymbol{\psi}_t} \Pr(F_t|\boldsymbol{\Psi}_t = \boldsymbol{\psi}_t)\, p(\boldsymbol{\psi}_t) \tag{1}$$

Information on the deteriorating box girder obtained through inspections is included in the calculation of the probability of structural collapse through Bayesian updating of $p(\boldsymbol{\psi}_t)$ on the basis of the DBN model. The updated probability of structural collapse of the box girder is given by

$$\Pr(F_t|\mathbf{Z}_{0:t} = \mathbf{z}_{0:t}) = \sum_{\boldsymbol{\psi}_t} \Pr(F_t|\boldsymbol{\Psi}_t = \boldsymbol{\psi}_t)\, p(\boldsymbol{\psi}_t|\mathbf{z}_{0:t}) \tag{2}$$

where $p(\boldsymbol{\psi}_t|\mathbf{z}_{0:t})$ is the updated joint distribution of the deterioration state of the box girder and $\mathbf{Z}_{0:t} = \mathbf{z}_{0:t}$ is a set of all inspection outcomes in the time period $[0, t]$ related to the deterioration state of the box girder.

3 CONDITION MODEL

3.1 *Modeling of chloride-induced reinforcement corrosion*

The process of chloride-induced reinforcement corrosion consists of two phases: an initiation phase and a propagation phase. These phases are illustrated in Figure 2. During the initiation phase chlorides migrate from the concrete surface into the concrete. This process is described by a diffusion model. Corrosion of the reinforcement at depth W initiates

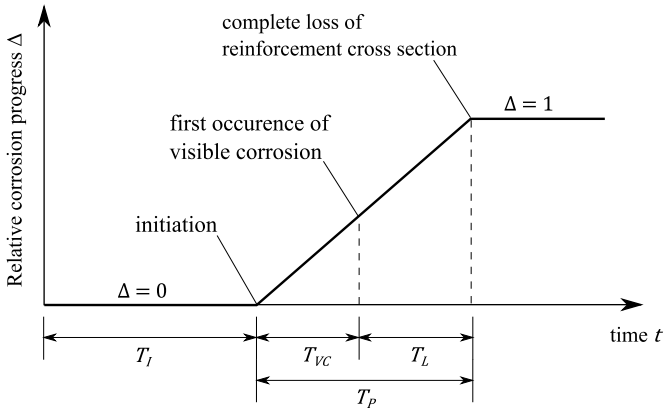

Figure 2. Phases of chloride-induced reinforcement corrosion (see Straub et al., 2009).

when a critical chloride concentration C_{cr} is exceeded. Following DuraCrete (2000), the time to initiation of reinforcement corrosion T_I is given by:

$$T_I = X_I \cdot \frac{W^2}{4D}\left(\mathrm{erf}^{-1}\left(1 - \frac{C_{cr}}{C_S}\right)\right)^{-2} \tag{3}$$

where D is the diffusion coefficient, C_s is the chloride concentration on the concrete surface, X_I represents the model uncertainty associated with T_I and $\mathrm{erf}(\cdot)$ is the Gauss error function. W, D, C_{cr}, C_s and X_I are here modeled as lognormal distributed random variables (Straub et al., 2009, Qin and Faber, 2012).

The limit state function (LSF) for corrosion initiation at time t can be written as:

$$g_{CI}(t) = T_I - t \tag{4}$$

The propagation phase is modeled by a simplified linear model as indicated in Figure 2 following Straub et al. (2009). The model describes the corrosion progress at time t in terms of the relative corrosion progress $\Delta_t = \Delta(t)$ as:

$$\Delta_t = \Delta(t) = \begin{cases} 0, & t \le T_I \\ \dfrac{1}{T_P}(t - T_I), & T_I < t \le T_P + T_I \\ 1, & t > T_P + T_I \end{cases} \tag{5}$$

where T_P is the period from corrosion initiation to complete loss of cross-sectional area of the reinforcement. The remaining cross-sectional area of the reinforcement at time t, $A_t = A(t)$, is given by:

$$A_t = A(t) = (1 - \Delta_t)\, A_0 \tag{6}$$

where A_0 is the initial cross-sectional area of the reinforcement.

The propagation phase T_P is divided into two separate phases as shown in Figure 2. The period from corrosion initiation to first occurrence of visible corrosion (e.g. stains of corrosion on the concrete surface and cracks) is denoted by T_{VC}. The remaining period to complete loss of the cross-

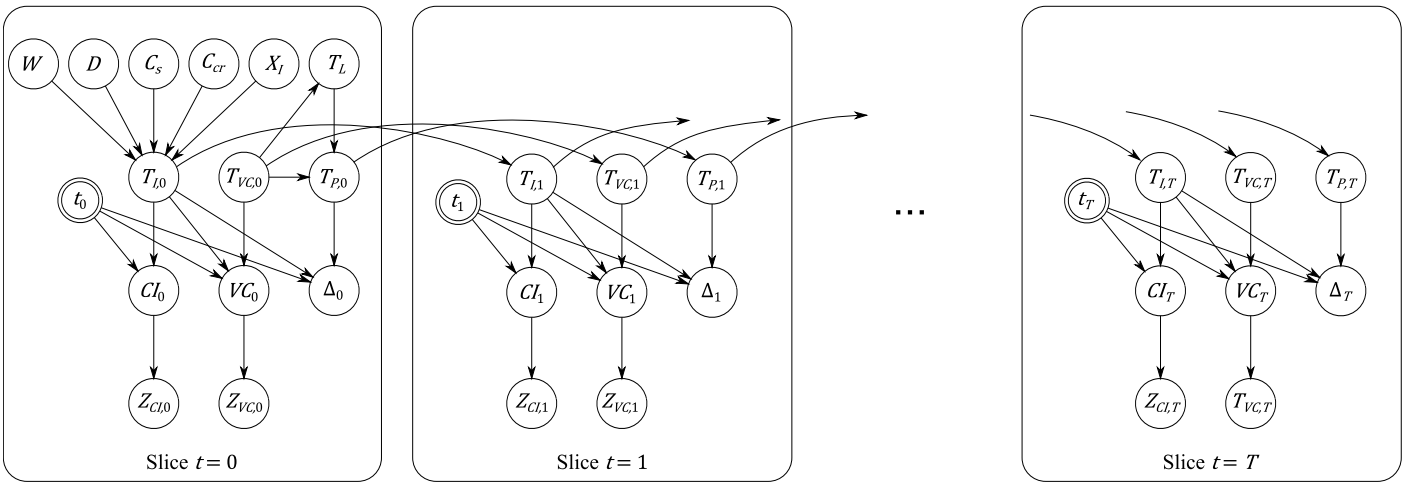

Figure 3. DBN model of chloride-induced reinforcement corrosion.

sectional area of the reinforcement is denoted by T_L. T_P is consequently written as:

$$T_P = T_{VC} + T_L \tag{7}$$

The periods T_{VC} and T_L are modeled as correlated lognormal distributed random variables.

The LSF for visible corrosion can be written as:

$$g_{VC}(t) = T_I + T_{VC} - t \tag{8}$$

Based on Equations (3) to (8), it is possible to construct a DBN model of chloride-induced reinforcement corrosion as shown in Figure 3. The DBN model consists of $t = 0,1,2 \dots, T$ time slices. Each time slice represents the state of the corrosion process at the end of the year t. Nodes d, D, C_S, C_{cr}, X_I, T_L, $T_{I,t}$, $T_{VC,t}$ $T_{P,t}$ and Δ_t $(t = 0, \dots, T)$ represent continuous random variables. These variables are discretized following the discretization scheme proposed by Straub (2009). Node CI_t $(t = 0, \dots, T)$ describes the event of corrosion initiation at year t. It has two discrete states: initiation or no initiation (of corrosion). Node VC_t $(t = 0, \dots, T)$ represents the event of visible corrosion. It is a binary state variable indicating whether there is visible corrosion. The nodes t are deterministic nodes whose values are the years represented by the corresponding slice.

The conditional probability tables (CPTs) associated with the root nodes of the DBN are calculated based on the prior probability density functions (PDFs) of the corresponding random variables. $p(T_{I,0}|d, D, C_s, C_{cr}, X_I)$ is determined based on Equation (3) using Monte Carlo simulation following Straub (2009). $p(T_L|T_{VC,0})$ is computed from the bivariate lognormal distribution. $p(T_{P,0}|T_{VC,0}, T_L)$ is constructed based on Equation (7). The CPTs $p(T_{I,t}|T_{I,t-1})$, $p(T_{VC,t}|T_{VC,t-1})$ und $p(T_{P,t}|T_{P,t-1})$ $(t = 1, \dots, T)$ are unit matrices since $T_{I,t}$, $T_{VC,t}$ and $T_{P,t}$ are time-invariant. $p(CI_t|t, T_{I,t})$ $(t = 0, \dots, T)$ is determined based on the LSF defined by Equation (4). It follows that $\{CI_t = \text{initiation}\}$ if $g_{CI}(t) \leq 0$ and $\{CI_t = \text{no initiation}\}$ if $g_{CI}(t) > 0$. Similarly, $p(VC_t|t, T_{VC,t})$ is constructed based on the LSF given by Equation (8). It follows that $\{VC_t = \text{visible corrosion}\}$ if $g_{VC}(t) \leq 0$ and $\{VC_t = \text{no visible corrosion}\}$ if $g_{VC}(t) > 0$. The CPT $p(\Delta_t|t, T_{I,t}, T_{P,t})$ is constructed based on Equation (5).

3.2 *Modeling of inspections*

Two inspection methods are considered: half-cell potential measurements and visual inspections of concrete surfaces. These inspections methods provide information on the actual progress of reinforcement corrosion. This information can be used to update the deterioration model.

Half-cell potential measurements provide information about the state of corrosion initiation CI_t. The outcome of a half-cell potential measurement at time t is modeled by a random variable $Z_{CI,t}$ with two discrete states: indication or no indication (of corrosion initiation). The quality of half-cell potential measurements is described by the likelihood function $p(Z_{CI,t}|CI_t)$ which quantifies the probability of obtaining an inspection result $Z_{CI,t}$ for a given state of corrosion initiation CI_t (Faber et al., 2006). The likelihood function of the half-cell potential measurement $p(Z_{CI,t}|CI_t)$ is fully defined by the probability of detection PoD_{CI} and the probability of false alarm $PoFA_{CI}$ as shown in Table 1. The results of half-cell potential measurements are integrated into the DBN model by including nodes $Z_{CI,t}$ in every time slice $t = 0, \dots, T$ which directly depend on the corresponding nodes CI_t as depicted in Figure 3. The CPTs associated with nodes $Z_{CI,t}$ are fully defined by the likelihood function $p(Z_{CI,t}|CI_t)$.

Visual inspections provide accurate information about the state of visible corrosion VC_t. The outcome of a visual inspection at time t is represented

Table 1. Likelihood function $p(Z_{CI,t}|CI_t)$ modeling the quality of half-cell potential measurements.

	CI_t = initiation	CI_t = no initiation
$Z_{CI,t}$ = indication	PoD_{CI}	$PoFA_{CI}$
$Z_{CI,t}$ = no indication	$1 - PoD_{CI}$	$1 - PoFA_{CI}$

by a binary random variable $Z_{VC,t}$ with states detection or no detection (of visible corrosion). The likelihood function $p(Z_{VC,t}|VC_t)$ describing the quality of visual inspections is also completely defined by the probability of detection $PoD_{VC} = p(Z_{VC,t} = \text{detection}|VC_t = \text{visible corrosion})$ and the probability of false alarm $PoFA_{VC} = p(Z_{VC,t} = \text{detection}|VC_t = \text{no visible corrosion})$. Following Faber et al. (2006), visual inspections are assumed to be perfect, i.e. $PoD_{VC} = 1$ and $PoFA_{VC} = 0$. Analogous to half-cell potential measurements, the results of visual inspections are included in the DBN model by defining nodes $Z_{VC,t}$ with parent nodes VC_t in each time slice $t = 0, \dots, T$ (see Figure 3). The corresponding CPTs are fully defined by the likelihood function $p(Z_{VC,t}|VC_t)$.

3.3 *Spatial model of chloride-induced reinforcement corrosion*

As previously mentioned, the box girder is divided into sections which are further divided into elements. The corrosion progress of these elements is generally correlated due to common uncertain influencing factors such as common environmental conditions and material characteristics. Following Faber et al. (2006) and Straub et al. (2009) elements with common exposure conditions and material characteristics are grouped into zones. It is assumed that there is no interdependence between different zones. As an example, elements making up the bridge deck may belong to one zone as they are exposed to similar levels of chlorides.

The size of the elements is determined by the length of the sections as described in Section 2. The choice of the length of the sections has to take the spatial variation of the relevant parameters influencing the deterioration process into account. In accordance with Faber et al. (2006) and Straub et al. (2009), the length of the sections shall be less than the correlation lengths of the relevant influencing factors. This approach ensures that within each element the influencing parameters are strongly correlated. They may, therefore, be approximated by a single random variable within each element. Hence, the progress of chloride-induced reinforcement corrosion of individual elements may be computed using separate DBN models as introduced in Sections 3.1 and 3.2. Note that the current model does not take the spatial variation of the corrosion process around the circumference of the box girder into account. To properly account for this effect, each element should be further divided in the direction perpendicular to the longitudinal axis of the box girder such that the resulting rectangular elements have dimensions in the order of the correlation lengths of the relevant influencing factors.

The determination of the probabilistic model parameters of the random influencing factors within one zone (e.g. their mean and standard deviation) is subject to statistical uncertainty. This is caused by a limited amount of data or in some cases, the probabilistic models are derived using data from different structures. Within one zone the statistical uncertainty is identical for all elements. This introduces statistical dependence between the parameters influencing the deterioration of individual elements within one zone. Faber et al. (2006) propose to model these dependencies through random hyper-parameters. The parameters of the deterioration models of individual elements within one zone are independent given a certain realization of these hyper-parameters. In the context of chloride-induced reinforcement corrosion, the hyper-parameters may include the mean of the diffusion coefficient μ_D and the mean of the chloride concentration on the concrete surface μ_{C_s} (Faber et al., 2006).

Based on the above, it is possible to construct a global DBN model of chloride-induced reinforcement corrosion, which considers the spatial correlation of the deterioration behavior of the individual elements. Figure 4 illustrates the intra-slice topology (within a slice) of the initial time slice of the global DBN model. For clarity, this illustration considers only three elements of one zone. The parameters D and C_s of the individual deterioration models are connected through hyper-parameters μ_D and μ_{C_s}.

The global DBN model allows the computation of the joint distribution $p(\boldsymbol{\psi}_t)$ as well as the updated joint distribution $p(\boldsymbol{\psi}_t|\mathbf{z}_{0:t})$ of the uncertain system deterioration state $\boldsymbol{\Psi}_t$ at time t which is defined as:

$$\boldsymbol{\Psi}_t = \left[CI_{t,0}, VC_{t,0}, \Delta_{t,0}, \dots, CI_{t,m}, VC_{t,m}, \Delta_{t,m}\right]^T \quad (9)$$

where m is the total number of elements.

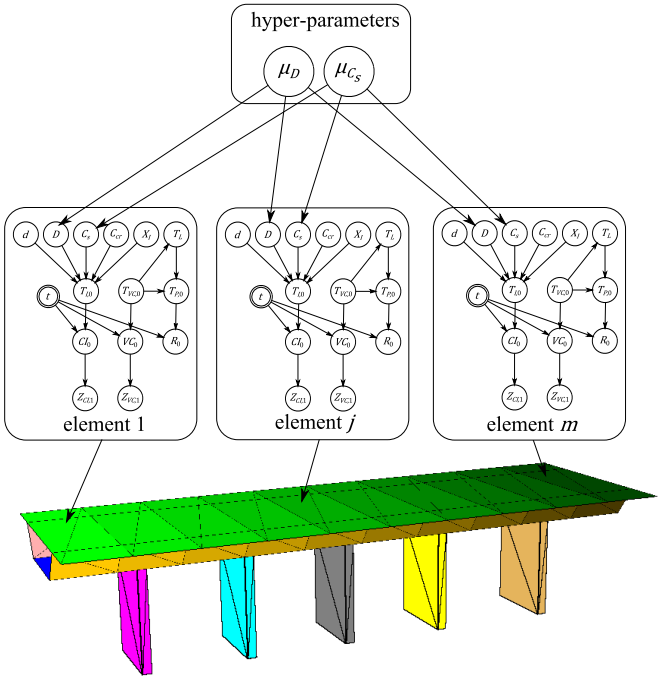

Figure 4. Intra-slice topology of the initial time slice $t = 0$ of the global DBN modeling the system deterioration of a box girder subjected to chloride-induced reinforcement corrosion.

4 STRUCTURAL MODEL

The probability of structural collapse of the box girder at time t conditional on a certain system deterioration state, $\Pr(F_t|\boldsymbol{\Psi}_t = \boldsymbol{\psi}_t)$, is estimated based on a simplified structural model. The following fundamental assumptions underlie the applied structural model: (a) the box girder is modeled as a continuous linear-elastic beam, (b) only global bending failure of the box girder is considered and (c) the box girder is modeled as a series system of cross-section failure events. This model can be extended to a more realistic and less conservative model.

The box girder is subjected to a random traffic load, which is here modeled by a spanwise uniformly distributed load whose annual maximum Q has the Gumbel distribution. Different traffic load cases are defined such that the bending moments at the centers of each span and at each support column are maximized.

Dead and prestressing loads are modeled as deterministic parameters, and so are the material and geometrical properties of the box girder. Therefore, a deterministic maximum plastic bending resistance of each cross-section along the box girder can be computed as a function of a given deterioration state $\boldsymbol{\Psi}_t = \boldsymbol{\psi}_t$. For this purpose, the cross-sectional area of the reinforcement associated with each element of the condition model is reduced according to the deterioration state $\boldsymbol{\Psi}_t = \boldsymbol{\psi}_t$.

With the structural model modified according to the deterioration state $\boldsymbol{\Psi}_t = \boldsymbol{\psi}_t$, it is possible to determine a maximum traffic load $q_{max}(\boldsymbol{\psi}_t)$ which can be withstood by the damaged box girder. Subsequently, the probability of structural collapse of the box girder at time t conditional on a certain system deterioration state $\boldsymbol{\Psi}_t = \boldsymbol{\psi}_t$ can be calculated as:

$$\Pr(F_t|\boldsymbol{\Psi}_t = \boldsymbol{\psi}_t) = 1 - F_Q\big(q_{max}(\boldsymbol{\psi}_t)\big) \qquad (10)$$

where $F_Q(\cdot)$ is the distribution of the annual maximum of the traffic load Q.

5 SOFTWARE PROTOTYPE

The software prototype consists of two parts: a front-end with a graphical user interface (GUI) implemented in Java and a back-end implemented in Matlab. The front-end provides the functionality required for defining the condition model, enter inspection data and visualize assessment results. The back-end is the computational core of the software prototype. The architecture of the software prototype is illustrated in Figure 5.

The GUI is divided into two panels as shown in Figure 6. The upper panel contains a rotatable 3D model of the box girder. The data required for the 3D representation is stored in an XML file called

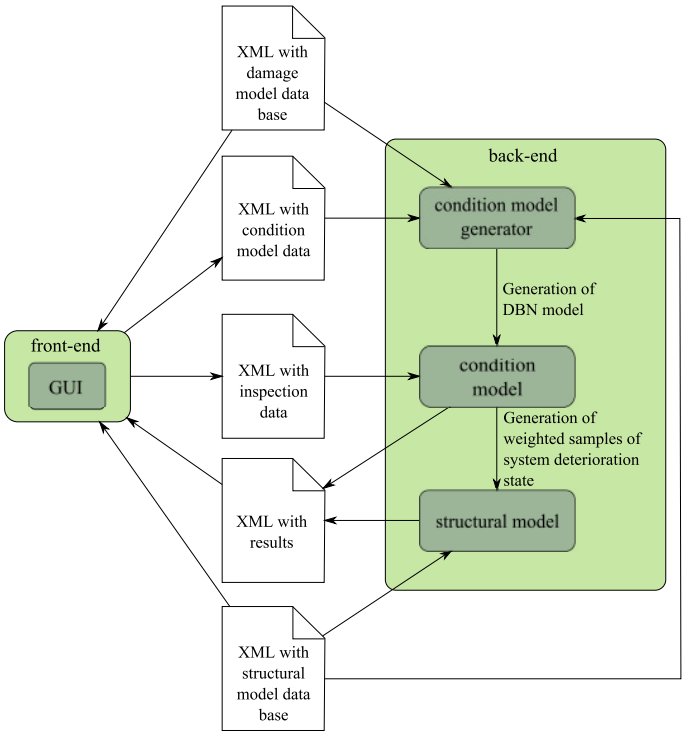

Figure 5. Architecture of the software prototype.

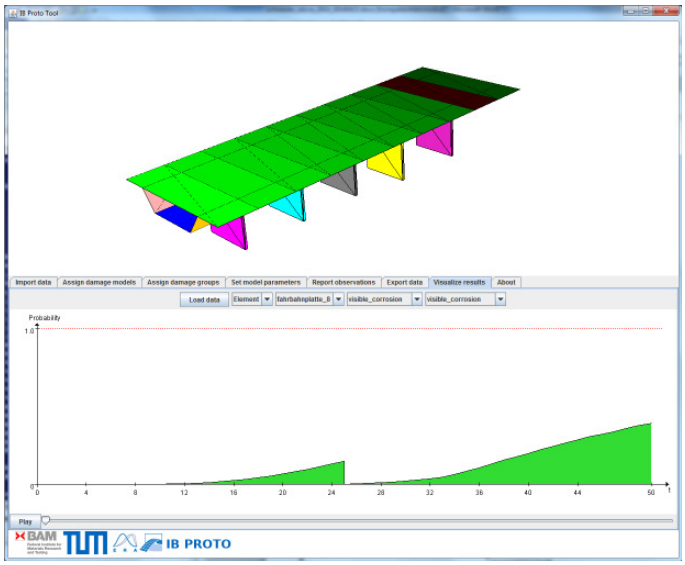

Figure 6. Screenshot of front-end (GUI).

structural model data base (see Figure 5). This file also provides information on size and location of the individual sections of the girder. The lower panel provides different tabs for entering and visualizing model data. The user can assign relevant deterioration models to each element if the "assign damage models" tab is active. Possible deterioration models are defined in a damage model data base (see Figure 6). (Note that currently only chloride-induced reinforcement corrosion is available. It is intended to extend the software to include further deterioration processes.) The "assign damage groups" tab provides a table that allows the user to define groups of elements. Each group represents one zone as described in Section 3.3. The user may set the parameters of the deterioration models in a table provided in the "set model parameters" tab. The condition model data (deterioration model assignments, group defini-

tions, and parameter data) can be exported to an XML file as indicated in Figure 5. Inspection results providing information on the condition of any of the elements can be entered if the "report observations" tab is active. The inspection results can be exported to an XML file (see Figure 5).

The back-end consists of three modules as indicated in Figure 5. The first module generates a condition model as described in Section 3 based on the condition model data, the deterioration model data base (default deterioration model data), and the structural model data base (service-life). The second module (the condition model) implements an inference algorithm for computing the updated joint distribution $p(\boldsymbol{\psi}_t|\mathbf{z}_{0:t})$ of the uncertain system deterioration state $\boldsymbol{\Psi}_t$ based on the DBN model. Currently, the likelihood weighting algorithm is implemented (e.g. Russell and Norvig, 2010). This algorithm generates weighted samples of $\boldsymbol{\Psi}_t$ which are consistent with the inspection results $\mathbf{Z}_{0:t} = \mathbf{z}_{0:t}$. The weights reflect the likelihood that the samples accord to the inspection results. The third module implements the structural model described in Section 4. The required data for initializing the structural model is contained in the structural model data base (geometry, material and load data). The model computes the updated probability of structural collapse of the box girder at time t based on the weighted samples of $\boldsymbol{\Psi}_t$ as follows:

$$\Pr(F_t|\mathbf{Z}_{0:t} = \mathbf{z}_{0:t}) \approx \frac{\sum_{k=1}^{n_{sim}} \Pr\left(F_t|\boldsymbol{\Psi}_t = \boldsymbol{\psi}_t^{(k)}\right) \cdot w_t^{(k)}}{\sum_{k=1}^{n_{sim}} w_t^{(k)}} \quad (11)$$

where $\boldsymbol{\psi}_t^{(k)}$ is the kth sample of $\boldsymbol{\Psi}_t$, $w_t^{(k)}$ is the corresponding weight and n_{sim} is the total number of samples. The computed results (deterioration state and reliability) are exported to an XML file (see Figure 5). These results can be imported and visualized in the "visualize results" tab of the GUI (see Figure 6).

6 CASE STUDY

For the purpose of illustration, the software prototype is applied to a 352 m long and 24.5 m wide highway bridge with a service life of 50 years. The superstructure of the bridge is a continuous single-cell prestressed concrete box girder with six spans. A schematic of the box girder is shown in Figure 7. The ultimate global bending resistance of the undamaged box girder as a function of the position x along the girder is given in Figure 8. The parameters of the Gumbel distribution describing the annual maximum Q of the traffic load are selected such that the undamaged box girder has a reliability index

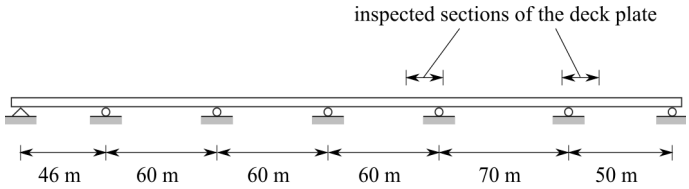

Figure 7. Schematic of the box girder indicating the inspected sections of the deck plate.

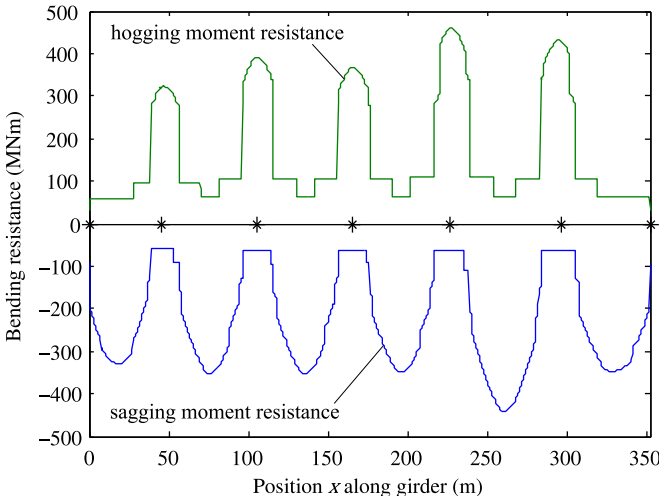

Figure 8. Ultimate global bending resistance of the box girder.

$\beta = 4.7$ with a one-year reference period. The calibration assumes a coefficient of variation $\delta_Q = 0.3$.

The box girder is subjected to chloride attack due to the application of deicing salt. To model the deterioration state, the box girder is divided into $n = 176$ sections with lengths of 2 m. This discretization scheme assumes a correlation length of the relevant influencing parameters $l_X = 2$ m. The deck plate of the box girder is assumed to be exposed to a higher chloride surface concentration than the webs and the bottom flange. Based on this assumption, the elements comprising the deck plate are grouped into one zone (zone 1) and all other elements are grouped into another zone (zone 2). The probabilistic models of the parameters of the corrosion model for all elements of the condition model are listed in Table 2.

Table 2. Probabilistic models of the parameters of the corrosion model for all elements of the condition model (DuraCrete, 2000, Faber et al., 2006).

Variable	Distribution	Mean	CoV	Correlation
W (mm)	LN	40	0.2	
D (mm^2/yr)	LN	μ_D	0.5	
C_s (wt.%)[a]	LN	μ_{C_s}	0.4	
C_{cr} (wt.%)[a]	LN	0.8	0.125	
X_I (-)	LN	1.0	0.05	
T_{VC}, T_L (yr)	Bi-LN	(12;38)	(0.3;0.3)	$\rho = 0.9$
μ_D (mm^2/yr)	N	20	0.1	
μ_{C_s}[b] (wt.%)[a]	N	1.5	0.1	
μ_{C_s}[c] (wt.%)[a]	N	1.0	0.1	

[a] weight-percent of cement
[b] zone 1 (deck plate)
[c] zone 2 (webs and bottom flange)

Two 20-m-long sections of the deck plate between $x = 210$ m and $x = 230$ m as well as $x = 290$ m and $x = 310$ m are visually inspected at time $t = 25$ years. The inspected sections are indicated in Figure 7. It is assumed that none of the inspected elements show signs of visible corrosion. In addition to visual inspection, half-cell potential measurements of these sections are performed at the same time. Following Straub et al. (2009), a $PoD_{CI} = 0.9$ and a $PoFA_{CI} = 0.29$ are selected to model the quality of the half-cell potential measurements. It is assumed that the half-cell potential measurements result in no indication of corrosion initiation for all inspected elements.

Figure 9 shows the computed prior probability of corrosion initiation and visible corrosion. The computed probabilities of corrosion initiation and visible corrosion of all elements in zone 1 (deck plate) are higher than the corrosion probabilities of the elements in zone 2 (webs and bottom flange). This result is expected since the elements in zone 2 are exposed to a lower surface concentration of chlorides.

Figure 10 shows the influence of the inspection results on the probability of corrosion initiation and visible corrosion of inspected and uninspected elements in zone 1. The small influence of the inspection results on the corrosion probabilities of the uninspected elements follows from the low resulting correlation between the diffusion coefficients and chloride surface concentrations implied by the applied hierarchical dependence model. It can be shown that the resulting coefficient of correlation among the chloride surface concentrations is $\rho_{C_s} = 0.06$ and the resulting coefficient of correlation among the diffusion coefficients is $\rho_D = 0.04$ in zone 1.

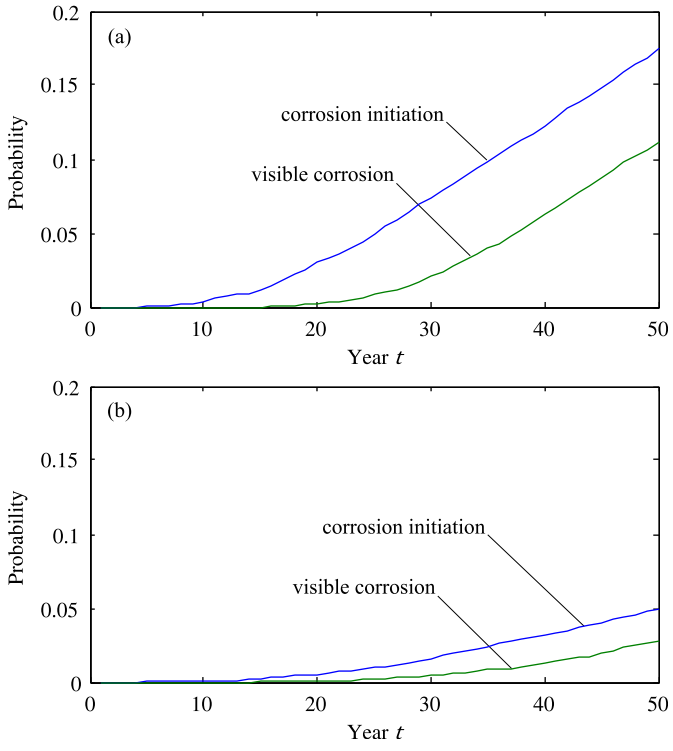

Figure 9. Prior probability of corrosion initiation and visible corrosion: (a) elements in zone 1 (deck plate); (b) elements in zone 2 (webs and bottom flange).

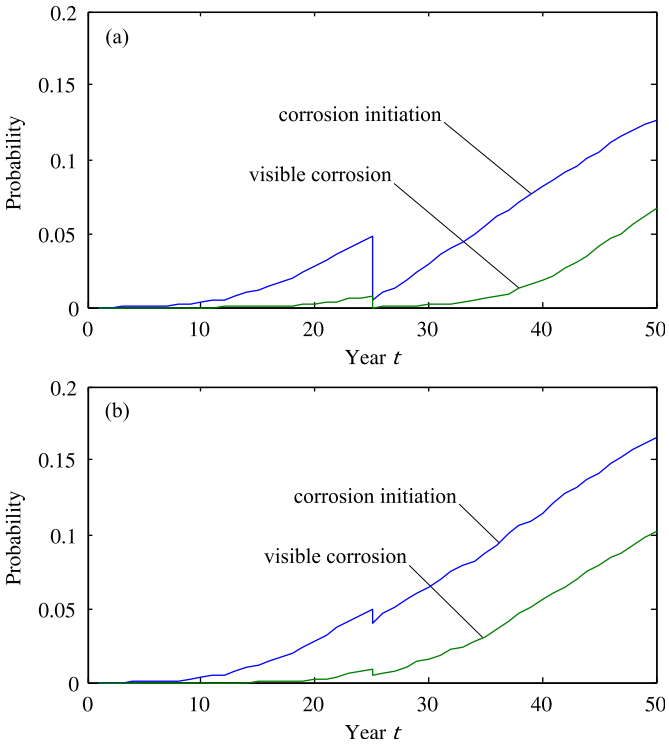

Figure 10. Updated probability of corrosion initiation and visible corrosion of all elements in zone 1: (a) inspected elements in zone 1 (inspection result = no visible corrosion and no indication of corrosion initiation through HCPM at $t = 25$ years); (b) uninspected elements in zone 1.

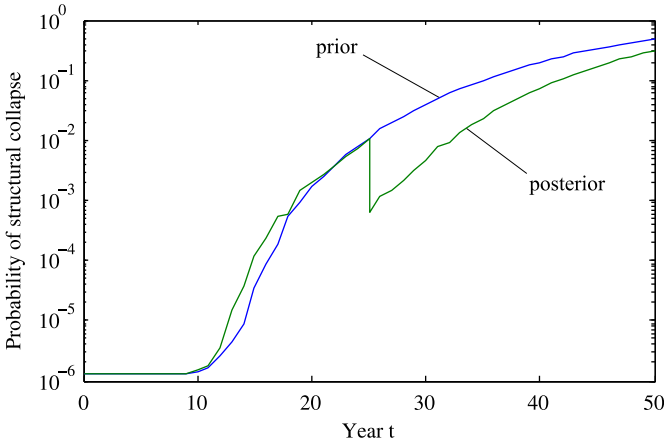

Figure 11. Prior and posterior probability of structural collapse.

Figure 11 shows the computed prior and posterior probability of structural collapse. The effect of the inspection results on the probability of structural collapse is relatively large even though only a small portion of the bridge is inspected. This result is because the inspected areas of the deck plate are in the vicinity of two critical cross-sections of the box girder which have a significant effect on the system reliability estimate.

The predicted probabilities of structural collapse are relatively high. These results are attributed to the simplified structural model which does not account for the structural redundancy of the continuous box girder. The high probabilities of structural collapse are also due to the simplified corrosion propagation

model and, possibly, the simplified discretization scheme.

7 CONCLUDING REMARKS

This paper presents a system model for assessing the reliability of prestressed concrete box girders subjected to chloride-induced corrosion. The deterioration state of a deteriorating box girder is modeled based on a DBN model that accounts for the spatial variation of the corrosion process by a hierarchical model. The structural reliability of a deteriorating box girder is assessed by combining the deterioration model with a structural model. Information on the deterioration state of a box girder obtained through inspections is included in the system reliability assessment through Bayesian updating on the basis of the DBN model.

The developed software prototype provides the functionality for performing computations on the basis of the described system model (i.e. the deterioration model and structural model). The software can be run by non-experts using the graphical user interface which facilitates the definition of the system deterioration model, inspection data input and visualization of assessment results. The graphical user interface was coupled with a back-end which is the computational core of the software prototype. The back-end implements the likelihood weighting algorithm for performing Bayesian inference on the basis of the DBN model. However, the performance of this algorithm rapidly degrades with an increasing number of inspection results. We are currently working on identifying and implementing a more efficient algorithm.

The software prototype was applied to a case study of a typical highway bridge with six spans to demonstrate the effect of partial inspections on the system reliability. The case study illustrated that it is possible to infer the condition of uninspected parts of the structure due to the spatial correlation of the corrosion process. It was, however, shown that the currently implemented corrosion model may underestimate the spatial correlation of the corrosion process. In addition, the corrosion propagation model may oversimplify the underlying physical process. Furthermore, the proposed discretization scheme does not account for the spatial variation of the corrosion process around the circumference of the box girder. These aspects require further research.

ACKNOWLEDGEMENT

This work was performed as part of project FE 15.0546/2011/LRB (Schneider et al., 2014) funded by BASt Federal Highway Research Institute, Germany.

REFERENCES

DuraCrete (2000) Statistical quantification of the Variables in the Limit State Functions. DuraCrete: Probabilistic Performance Based Durability Design of Concrete Structures. The European Union – Brite EuRam III (Project BE95-1347/R9).

Faber, M. H., Straub, D. & Maes, M. A. (2006) A computational framework for risk assessment of RC structures using indicators. Computer-Aided Civil and Infrastructure Engineering, 21, 216-30.

Murphy, K. P. (2002) Dynamic Bayesian Networks: Representation, Inference and Learning. University of California, Berkley.

Qin, J. & Faber, M. H. (2012) Risk Management of Large RC Structures within a Spatial Information System. Computer-Aided Civil and Infrastructure Engineering, 27, 385–405.

Russell, S. J. & Norvig, P. (2010) Artificial Intelligence - A Modern Approach, Prentice Hall.

Schneider, R., Fischer, J., Bügler, M., Thöns, S., Borrmann, A. & Straub, D. (2014) Intelligente Bauwerke – Prototyp zur Ermittlung der Schadens- und Zustandsentwicklung für Elemente des Brückenmodells. Berichte der Bundesanstalt für Straßenwesen, Brücken- und Ingenieurbau (in print). in German.

Straub, D. (2009) Stochastic modeling of deterioration processes through dynamic Bayesian networks. Journal of Engineering Mechanics, 135, 1089-1099.

Straub, D. & Der Kiureghian, A. (2011) Reliability acceptance criteria for deteriorating elements of structural systems. Journal of Structural Engineering, 137, 1573-1582.

Straub, D., Malioka, V. & Faber, M. H. (2009) A framework for the asset integrity management of large deteriorating concrete structures. Structure and Infrastructure Engineering, 5, 199-213.